Philosophical Magazine

ISSN: 1478-6435 (Print) 1478-6443 (Online) Journal homepage: https://www.tandfonline.com/loi/tphm20

Phase transition of ZrN under pressure

Murat Durandurdu

To cite this article: Murat Durandurdu (2019) Phase transition of ZrN under pressure, Philosophical Magazine, 99:8, 942-955, DOI: 10.1080/14786435.2019.1566797

To link to this article: https://doi.org/10.1080/14786435.2019.1566797

Published online: 14 Jan 2019.

PHILOSOPHICAL MAGAZINE
2019, VOL. 99, NO. 8, 942–955
https://doi.org/10.1080/14786435.2019.1566797

Taylor & Francis
Taylor & Francis Group

Phase transition of ZrN under pressure

Murat Durandurdu

Department of Materials Science & Nanotechnology Engineering, Abdullah Gül University, Kayseri, Turkey

ABSTRACT

A first principles constant pressure approach is carried out to probe the high-pressure behaviour of the rocksalt (RS) structured zirconium nitride (ZrN). The existence of first order reconstructive phase transition from the RS crystal to a CsCl-type crystal is, for the first time, established throughout the simulations. Upon decompression, the CsCl type phase converts back to the original RS structure by following the same transformation mechanism, suggesting a reversible phase transformation in ZrN. The RS-to-CsCl phase change is additionally considered through the thermodynamic theorem and projected to take place at around 225 GPa in experiments. The structural parameters and mechanical properties computed are found to be comparable with some of the previous findings. Additionally, we investigate the response of ZrN to uniaxial compression and tension stresses. The uniaxial stresses initially lead to a tetragonal modification of the simulation box having an I4/mmm symmetry and subsequently structural failure that is expected to occurs at about −10 and 15 GPa in experiments.

ARTICLE HISTORY
Received 29 June 2018
Accepted 4 December 2018

KEYWORDS
Ceramics; density-functional theory; molecular dynamic simulations; phase transitions

1. Introduction

Group IVB transition metal nitrides, promising engineering materials, have been drawn considerable attentions due to their various high tech applications. They possess an unusual bonding character (a mixture of ionic, covalent and metallic bonding) [1–4], and hence they acquire metallic and non-metallic features, for example, extreme hardness and high melting points like covalent material and conductivity and even in some cases superconductivity like metals. Such a bonding character is believed to be indeed responsible for their astonishing mechanical and chemical properties [5–13], which lead to various high-tech applications such as microelectronics, magnetic recording, corrosion, cutting tools, low-temperature fuel cells, resistant coating, optoelectronic devices, etc.

Amongst group IVB transition metal nitrides, zirconium nitrides can form various crystalline phases (ZrN, ZrN_x, Zr_3N_4, etc.) [14–20]. These crystalline

CONTACT Murat Durandurdu murat.durandurdu@agu.edu.tr, mdurandurdu@gmail.com Department of Materials Science & Nanotechnology Engineering, Abdullah Gül University, Kayseri 38080, Turkey

phases and their physical properties are not fully understood yet. ZrN has the rocksalt (RS) crystal structure with space group Fm3 m. In this crystal, N concentration may change approximately from 22 to 50 at.%. Of course, depending on N concentration it can show different physical and mechanical properties. ZrN can offer numerous technological applications due to its superior properties [21–25]. Yet some of its technological applications do indeed require a full understanding of this material under extremely high pressure and temperature conditions. To our knowledge, no experimental study has been performed to investigate the high-pressure behaviour of ZrN up to date but there have been considerable theoretical efforts to examine its structural stability and high-pressure behaviour [26–34]. These theoretical investigations have essentially focused on the CsCl-type phase as its high-pressure phase because the RS structured materials commonly adopt a CsCl-type state under pressure. Yet there are some discrepancies in the projection of stable structure, transition pressure, lattice parameters, transition volumes and mechanical properties of ZrN crystals in these studies.

We need to emphasise here that not all RS structured materials follow this typical transformation pathway at high pressure and instead some can adopt different crystalline structures [35–37]. Furthermore, it is possible to observe an isostructural phase transition in the RS structured materials such that at the critical pressure, a noticeably volume collapse can be witnessed with no symmetry modification as in TiN [38,39]. Therefore further reliable dynamical simulations or experimental investigations are undeniably desired to expose the true behaviour of ZrN under pressure.

The present work's main purpose is to uncover the high pressure phase of ZrN using a constant pressure *ab initio* method that can offer a solid suggestion regarding its high pressure behaviour and does not rely on any educated speculation about its high-pressure phase(s) on the contrary the thermodynamic theorem. Using the dynamical simulations, we confirm, for the first time, that ZrN does actually transform to a CsCl type structure. Such a phase change is projected to happen at about 225 GPa in experiments. We further suggest that the CsCl type structure is not quenchable to ambient conditions. Furthermore, we investigate its behaviour under uniaxial stresses and find that it shows structural failure. The failure is predicted to take place at around −10 GPa (tensile stress) and at 15 GPa (compressive stress). Our estimated parameters and mechanical properties accord fairly with some of the earlier studies.

2. Methodology

Quantum mechanical simulations in this study were executed within the generalised gradient approximation GGA [40,41] and norm-conserving nonlocal pseudopotentials [42] using the first-principles package SIESTA [43]. The DZP basis sets were chosen for the simulation. 150 Ry was used for the mesh

cutoff. The simulation box consisted of 216 atoms (108 Zr and 108 N atoms). The only Γ-point sampling of k-mesh was used. We executed molecular dynamics (MD) simulations using the NPH ensemble and applied the external pressure via the Parrinello and Rahman approach [44]. We compressed and tensioned the simulation box along the [1 0 0] direction and set primarily the other stress components to zero. For the energy–volume computations, we adopted the conventional cell with 8 atoms for the RS structure and 16 atoms for the CsCl type crystal and automatically generated $8 \times 8 \times 8$ and $6 \times 6 \times 6$ k-point mesh, respectively using Monkhorst and Pack [45]. KPLOT program [46] was used for symmetry investigation. This program provides all information (symmetry, lattice parameters, atomic position etc.) about of a given crystal structure. The symmetry investigation was performed within some tolerances such as 0.2 Å for bond lengths, 2° for bond angles and 0.7 Å for interplanar spacing.

3. Results

3.1 Hydrostatic compression

We primarily focus on the variation of volume obtained through the constant pressure first principles MD simulation to identify the thermodynamic description of pressure-induced phase transition in ZrN and present it in Figure 1. The volume smoothly decreases and at a pressure of 700 GPa it exhibits a severe

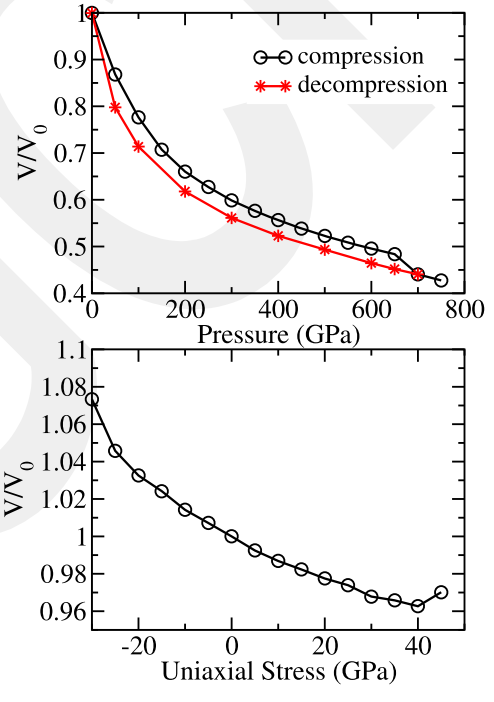

Figure 1. (a) Pressure–volume relation from the dynamical simulation. (b) Stress–volume relation.

decline. The volume drop is about 9%. This observation suggests the occurrence of a first-order phase transition in ZrN. Using the KPLOT program, we verify, for the first time, that ZrN indeed transforms from the RS structure to a CsCl type structure having $a = 2.196$ Å at this pressure. Upon decompression, the volume slowly increases and once the external pressure is changed from 50 and 0 GPa, it drastically increases and the original volume is recovered. The KPLOT examination reveals that the CsCl type structure alters back to the RS structure. This finding means that the CsCl type phase of ZrN is unquenchable, consisting of the earlier first principles phonon calculations in which it is found to be metastable at ambient pressure [33,34].

Because the amendment of the simulation box leads us to identify the transformation mechanism from the RS phase to CsCl type phase, which is a debate for a long time, we next probe the adjustment of the simulation cell parameters (lengths and angles) as a function of simulation step and show them in Figure 2. The supercell's lattice vectors, $\mathbf{L_1}$, $\mathbf{L_2}$, and $\mathbf{L_3}$, are along the [100], [010] and [001] directions, correspondingly. Up to the phase transition, all the cell vectors shrink with a similar magnitude and the cell angles remain almost 90°. On the other hand, during the phase change at 700 GPa, the simulation cell suffers severe reconstructions between 275 fs and 317 fs: all simulation cell lengths tend to increase and two angles change from 90° to 70° while the third one increases from 90° to 110°. The evolution of the CsCl-type phase is illustrated in Figure 3. This transformation

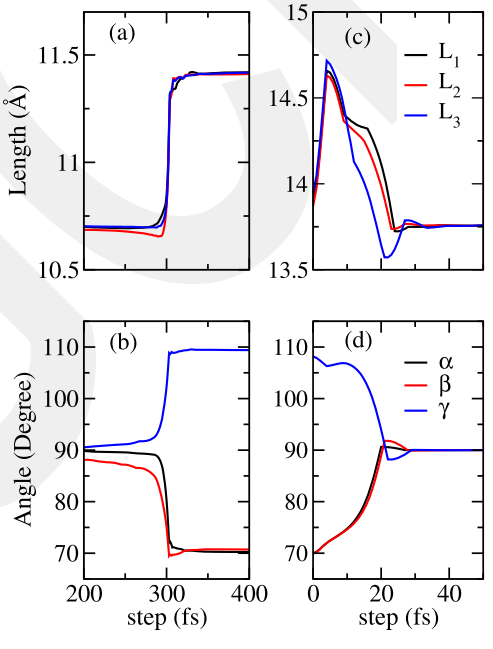

Figure 2. Modification of the simulation cell lengths and angles during the phase transformations. (a) and (b) at 700 GPa during compression. (c) and (d) at 0 GPa during decompression. α, β, and γ are the angle between the simulation cell vectors.

pathway is parallel to what has been perceived in the classical MD simulation of KCl [47]. Upon pressure release, the angles return to right angles and the cell lengths return to the original ones. This observation specifies that the RS-to-CsCl and CsCl-to-RS transitions follow exactly the same transformation pathway.

We carefully investigate the structures between 275 fs and 317 fs by the KPLOT program to see whether any intermediate phase is developed between the RS and CsCl-type structures but we could not identify any. At 310 fs, a CsCl type structure having $a = 2.196$ Å is identified. We perform similar analysis during the decompression from 50 to 0 GPa but again we could not detect any intermediate state. This is probably due to the occurrence of the phase transformation in a short simulation time scale that produces quite distorted states.

3.2 Thermodynamic theorem

The Parrinello–Rahman approach is indeed very successfully in replicating experimentally achieved high-pressure phases of materials or in proposing their new high-pressure structures. Yet the major cumbersome of this technique

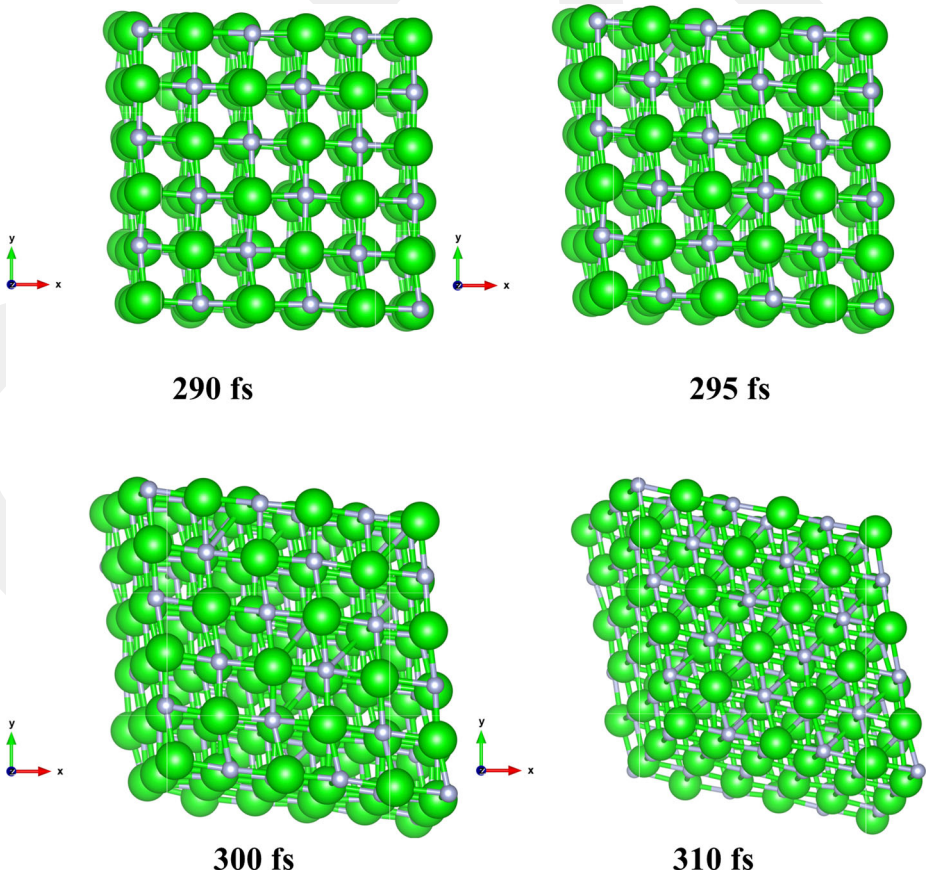

Figure 3. The evolution of CsCl structure at 700 GPa.

is the exaggerated transition pressure, relative to experiments. This is indeed related to some simulation conditions. There are no surface effects in simulated structures due to the application of periodic boundary conditions. There are no defects as well because of the use of an ideal structured. It should be pointed out here that pressure-induced phase transformations commonly nucleate and grow at defects and surfaces. No nucleation centres mean the occurrence of global (homogenous) phase transformations in simulations. Additionally the simulation time scale, too short relative to experiment, is another critical factor that can influence phase transformations. The short time refers a very fast pressurising or depressurising rate, which could not let sufficient time for the physical relaxation or reorganisations to occur, and might yield frozen states in simulations. All these factors in simulations push critical pressures to very higher values compared to experiments. Contrarily, the thermodynamic equation (Gibbs free energy $G = H - ST$) gives comparable transition pressures. Since the structural relaxation is performed at an absolute temperature, the Gibbs free energy becomes enthalpy ($H = E + PV$, where E, V and P represents energy, volume and external pressure, correspondingly). To estimate the enthalpy (H) we compute energy (E) of both RS and CsCl type crystals as a function of volume (V) and provide the $E-V$ curves in Figure 4. And then we fit the $E-V$ relations to the third-order Birch–Murnaghan equation of states (EOS)

$$E(V) = E_o + \frac{9V_OK}{16}\left\{\left[\left(\frac{V_O}{V}\right)^{\frac{2}{3}} - 1\right]^3 K' + \left[\left(\frac{V_O}{V}\right)^{\frac{2}{3}} - 1\right]^2 \left[6 - 4\left(\frac{V_O}{V}\right)^{\frac{2}{3}}\right]\right\}$$

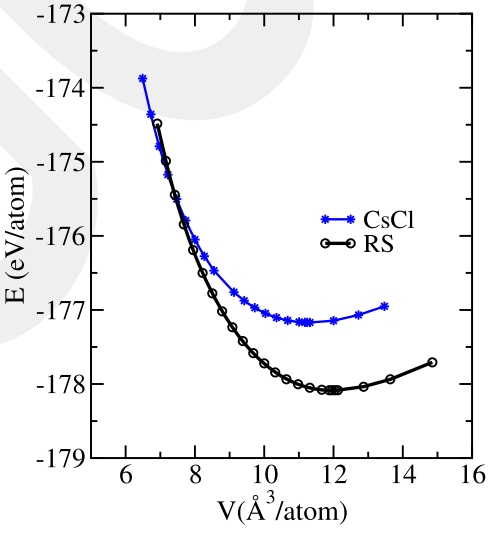

Figure 4. Energy–volume relation.

where E_0 and V_0 represent the zero pressure energy and volume, respectively, and K and K' is bulk modulus and its derivative respect to pressure, correspondingly. From the curve, we also estimate pressure ($P = -\mathrm{d}E/\mathrm{d}V$) and finally the H values. At zero temperature and a given pressure, the most stable phase has the lowest enthalpy. Because the crystals have the same H value at the structural phase change, the critical pressure can be straightforwardly estimated by equating H values of these two crystals. The H curves predicted are shown in Figure 5. The two curves cross at around 225 GPa, suggesting the occurrence of the RS-to-CsCl phase transformation at this pressure. Our estimated critical pressure accords with some of the previous first principles investigations as seen in Table 1.

The EOSs offer additional information about some important parameters of these crystalline phases as well. The EOSs yield the relative energy difference between the RS and CsCl type states to be ~0.91 eV/atom, comparable with the previous simulation results of 0.88 eV/atom [33]. The equilibrium volume of RS and CsCl type crystals is found to be 12.042 and 11.311 Å^3/atom, respectively.

3.3 Uniaxial stresses

The response of ZrN to uniaxial stresses, to our knowledge, has not been investigated in earlier reports. Considering the applications of ZrN in technology, it is indeed essential to understand its responses to finite strain. Therefore, in addition to hydrostatic pressure, we probe its behaviour under tensile and compressive stresses that are applied along [1 0 0] direction. The stress dependence of volume is provided in Figure 1 as well. The volume lessens with the increase of

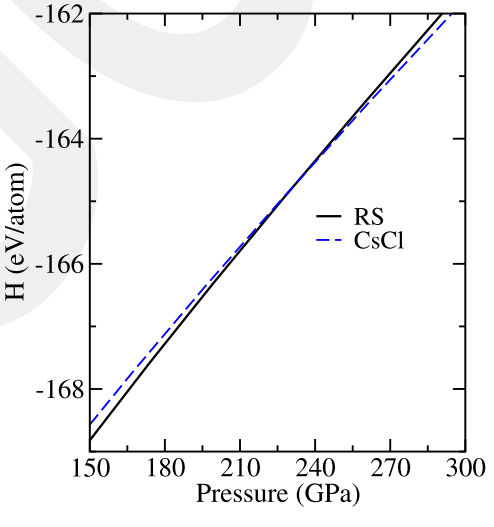

Figure 5. Variation of enthalpy under hydrostatic pressure.

Table 1. The equilibrium parameters of the RS and CsCl type crystals, P_t is transition pressure, K is bulk modulus, ν is Poisson's ratio, E is Young's modulus, μ is shear modulus and H_v is Vickers hardness.

Structure	a (Å)	P_t (GPa)	K (GPa)	ν	E(GPa)	μ(GPa)	H_v(GPa)	Ref.
RS	4.58	225	245	0.18	470	199	30[a]	Present
							31[b]	Present
							30[c]	Present
	4.63	339	238					[33]
	4.59	209						[34]
	4.57	98	250	0.24	376	154	26	[28]
	4.56		231	0.14	637	177		[27]
	4.56	333	231					[26]
	4.57		264					[32]
	4.57		248	0.23	396	152		[31]
	4.52		282	0.21	483	193		[31]
			215	0.16	443	160	17	[8]
			285	0.16	663	176		[8]
		94						[30]
CsCl	2.82		210					Present
	2.86		216					[33]
	2.88		225	0.29	281	109	15	[28]
	2.88		193					[26]

[a]Teter's equation
[b]Chen's equation
[c]Tian's equation

compressive uniaxial stress whereas it increases with the increase of tensile stress. The modification of volume under uniaxial stresses compared to the hydrostatic case is very small. This is a result of the simultaneous increase and decrease of the simulation cell vectors under uniaxial stresses (see Figure 6). Namely, the axis compressed (tensioned) decreases (increases) progressively whereas the other axes incline to expand (decline) since the material tries to reverse its volume. We should note here that under uniaxial stresses, the simulation cell vectors remain almost orthogonal. The simultaneous increase and decrease of the simulation cell vectors convert the structure from cubic to tetragonal with no change in coordination number. The tetragonal state has I4/mmm symmetry.

ZrN shows structural failure at −30 GPa (tensile) and at 45 GPa (compressive) in the present work as indicated by a volume expansion at these stresses. We believe that these critical values are overestimated as well. Yet we cannot unquestionably express the degree of the exaggeration in these critical stresses. Since the transition pressure for the hydrostatic case is overestimated a factor of about three times higher than the enthalpy calculation, by assuming the same degree of overestimation for the uniaxial cases, we can speculate that the structural failure of ZrN can occur at around −10 and 15 GPa in experiments.

3.4 Mechanical properties

Using the available data, we can effortlessly calculate some of the mechanical properties of ZrN. From the EOSs, the K value is predicted to be 245 GPa

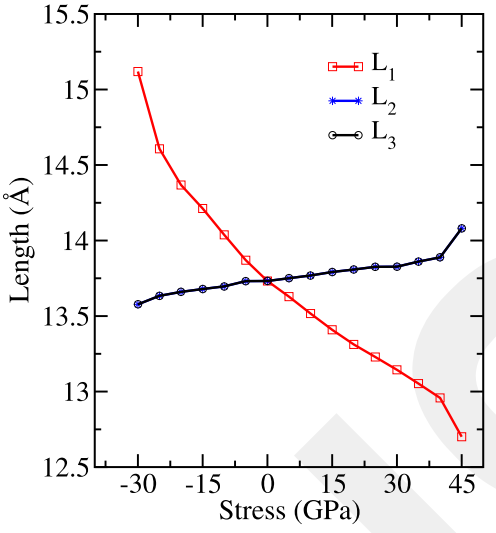

Figure 6. Modification of the simulation cell lengths under uniaxial stress.

(RS) and 210 GPa (CsCl). Our estimations reasonably agree with the experimental and some of the previous simulations data (see Table 1).

When a material is subjected to uniaxial stress, it experiences an expansion for compression and a reduction for tension in the lateral directions. Such a tendency can be explained by the Poisson's ratio (ν), which is one of the important elastic properties of a solid. The Poisson's ratio of a material exposed to a uniaxial stress is expressed as the negative ratio of lateral strain resultant from an applied strain and given by

$$\nu = -\frac{\varepsilon_{\text{lateral}}}{\varepsilon_{\text{applied}}}$$

where ε represents the strain. The variation of lateral strain ($\varepsilon_{\text{lateral}}$) as a function of applied strain ($\varepsilon_{\text{applied}}$) is demonstrated in Figure 7. From the best linear fitting line, the Poisson's ratio is predicted to be 0.18, in agreement with the earlier reports as seen in Table 1.

Since two elastic constants (bulk modulus and Poisson's ratio) are known, using the following equation,

$$E = 3K(1 - 2\nu)$$

we determine Young's modulus (E) to be 470 GPa for the RS state, according with again other calculations (Table 1).

We calculate the shear modulus (μ) using the following definition

$$\mu = \frac{E}{2(1+\nu)}.$$

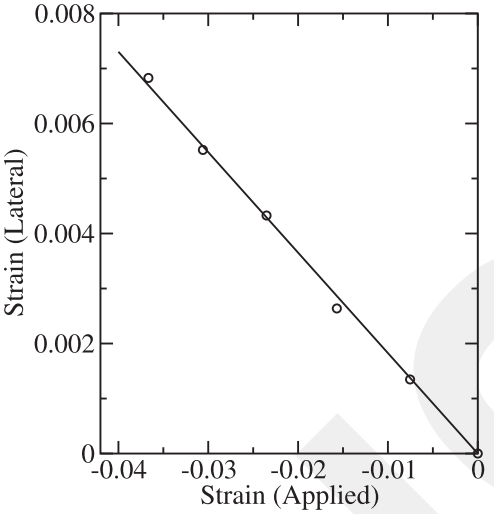

Figure 7. The variation of lateral strain as a function of applied strain for the RS phase.

The shear modulus of the RS structures is projected to be 199 GPa, slightly higher than the data available in the literature.

The Vickers hardness (H_v) is another mechanical property of interest. There have been considerable efforts to determine the correlation between H_v and elastic properties. These investigations have demonstrated the impact of shear and bulk modules on H_v and proposed some empirical relations. The first equation known as the Teter's equation suggests a linear relation between H_v and μ as follows [48]

$$H_v = 0.151\mu.$$

The second equation proposed by Chen [49] indicates a non-linear equation

$$H_v = 2\left(\frac{\mu}{n^2}\right)^{0.585} - 3\,(GPa)$$

where n is the Pugh's ratio ($n = K/\mu$). Later this equation was modified by Tian *et al.* [50] because the Chen's equation yields negative values for materials having small H_v values. The modified equation is given by

$$H_v = 0.92\left(\frac{1}{n}\right)^{1.137}(\mu)^{0.708}.$$

All these equations yield a value of about 30 GPa for the RS structure, which is indeed quite higher than the experimental result of 17 GPa (see Table 1).

4. Conclusions

We have executed a first principles constant pressure approach to uncover the high-pressure phase of the rocksalt (RS) structured ZrN and confirm that it undergoes a phase transition from the RS crystal to a CsCl-type crystal. On decompression, the CsCl type phase transforms back to the RS structure by following the same transformation pathway. We also perform the enthalpy calculations to investigate this phase change in details and estimate a critical pressure of about 225 GPa. Furthermore, we probe the behaviour of the ZrN under uniaxial compression and tension stresses and observe structural failure. The structural parameters and mechanical properties projected are found to be close to some of the other investigations.

Acknowledgements

The calculations were run on TÜBİTAK ULAKBİM, High Performance and Grid Computing Center (TRUBA resources).

Disclosure statement

No potential conflict of interest was reported by the author.

Funding

This is work was supported by the Abdullah Gül University Support Foundation.

References

[1] T.T. Oyama, *Introduction to the chemistry of transition metal carbides and nitrides*, in *The Chemistry of Transition Metal Carbides and Nitrides*, Springer, Dordrecht, 1996. pp. 1–27

[2] P. Blaha, J. Redinger and K. Schwarz, *Bonding study of TiC and TiN. II. theory*. Phys. Rev B 31 (1985), pp. 2316–2325.

[3] J. Häglund, A. Fernández Guillermet, G. Grimvall and M. Körling, *Theory of bonding in transition-metal carbides and nitrides*. Phys. Rev B. 48 (1993), pp. 11685–11691.

[4] V.P. Zhukov, V.A. Gubanov, O. Jepsen, N.E. Christensen and O.K. Andersen, *Calculated energy-band structures and chemical bonding in titanium and vanadium carbides, nitrides and oxides*. J. Phys. Chem. Solids 49 (1988), pp. 841–849.

[5] H. Holleck, *Material selection for hard coatings*. J. Vac. Sci. Technol. A 4 (1986), pp. 2661–2669.

[6] K. Inumaru, T. Ohara, K. Tanaka and S. Yamanaka, *Layer-by-layer deposition of epitaxial TiN–CrN multilayers on MgO (0 0 1) by pulsed laser ablation*. Appl. Surf. Sci. 235 (2004), pp. 460–464.

[7] D.J. Kim, Y.R. Cho, M.J. Lee, J.M. Hong, Y.K. Kim and K.H. Lee, *Properties of TiN–TiC multilayer coatings using plasma-assisted chemical vapor deposition*. Surf. Coat. Technol. 116 (1999), pp. 906–910.

[8] X. Chen, V.V. Struzhkin, Z. Wu, M. Somayazulu, J. Qian, S. Kung, A.N. Christensen, et al., *Hard superconducting nitrides*. Proc. Natl. Acad. Sci. Am. 102 (2005), pp. 3198–3201.
[9] A.J. Perry, *On the existence of point defects in physical vapor deposited films of TiN, ZrN, and HfN*. J. Vac. Sci. Technol. A 6 (1988), pp. 2140–2148.
[10] L. Hultman, *Thermal stability of nitride thin films*. Vacuum 57 (2000), pp. 1–30.
[11] I. Pollini, A. Mosser and J.C. Parlebas, *Electronic, spectroscopic and elastic properties of early transition metal compounds*. Phys. Rep. 355 (2001), pp. 1–72.
[12] L. Tsetseris, N. Kalfagiannis, S. Logothetidis and S.T. Pantelides, *Role of N defects on thermally induced atomic-scale structural changes in transition-metal nitrides*. Phys. Rev. Lett. 99 (2007), pp. 125503–125506.
[13] L.E. Toth, *Transition Metal Carbides and Nitrides, vol. 7 of Refractory Material Series*, Academic Press, New York, 1971.
[14] S. Yu, Q. Zeng, A.R. Oganov, G. Frapper, B. Huang, H. Niu and L. Zhang, *First-principles study of Zr–N crystalline phases: phase stability, electronic and mechanical properties*. RSC Adv. 7 (2017), pp. 4697–4703.
[15] M. Chhowalla and H.E. Unalan, *Thin films of hard cubic Zr3N4 stabilized by stress*. Nat. Mater. 4 (2005), pp. 317–322.
[16] L. Gribaudo, D. Arias and J. Abriata, *The N-Zr (nitrogen-zirconium) system*. J. Phase Equilib. 15 (1994), pp. 441–449.
[17] A. Zerr, G. Miehe and R. Riedel, *Synthesis of cubic zirconium and hafnium nitride having Th3P4 structure*. Nat. Mater. 2 (2003), pp. 185–189.
[18] P. Kroll, *Hafnium nitride with thorium phosphide structure: physical properties and an assessment of the Hf-N, Zr-N, and Ti-N phase diagrams at high pressures and temperatures*. Phys. Rev. Lett. 90 (2003), pp. 125501–125504.
[19] R. Juza, A. Gabel, H. Rabenau and W. Klose, *Über ein blaues Zirkonnitrid*. Z. Anorg. Allg. Chem. 329 (1964), pp. 136–145.
[20] W.H. Baur and M. Lerch, *On deciding between space groups Pnam and Pna21 for the crystal structure of Zr3N4*. Z. Anorg. Allg. Chem. 622 (1996), pp. 1729–1730.
[21] M. Burghartz, G. Ledergerber, H. Hein, R.R. Van der Laan and R.J.M. Konings, *Some aspects of the use of ZrN as an inert matrix for actinide fuels*. J. Nucl. Mater. 288 (2001), pp. 233–236.
[22] H. Randhawa, *Hard coatings for decorative applications*. Surf. Coat. Technol. 36 (1988), pp. 829–836.
[23] A. Singh, N. Kumar, P. Kuppusami, T.N. Prasanthi, P. Chandramohan, S. Dash, M.P. Srinivasan, E. Mohandas and A.K. Tyagi, *Tribological properties of sputter deposited ZrN coatings on titanium modified austenitic stainless steel*. Wear 280 (2012), pp. 22–27.
[24] S.M. Aouadi, M. Debessai and P. Filip, *Zirconium nitride/silver nanocomposite structures for biomedical applications*. J. Vac. Sci. Technol. B 22 (2004), pp. 1134–1140.
[25] R.W. Harrison and W.E. Lee, *Processing and properties of ZrC, ZrN and ZrCN ceramics: a review*. Adv. Appl. Ceram. 115 (2016), pp. 294–307.
[26] A. Srivastava, M. Chauhan and R.K. Singh, *Pressure induced phase transitions in transition metal nitrides: Ab initio study*. Phys. Status Solidi B 248 (2011), pp. 2793–2800.
[27] A. Srivastava and B.D. Diwan, *Structural and elastic properties of ZrN and HfN: ab initio study*. Can. J. Phys. 92 (2014), pp. 1058–1061.
[28] A.T.A. Meenaatci, R. Rajeswarapalanichamy and K. Iyakutti, *Pressure induced phase transition of ZrN and HfN: a first principles study*. J. At. Mol. Sci. 4 (2013), pp. 321–335.

[29] A. Hao, T. Zhou, Y. Zhu, X. Zhang and R. Liu, *First-principles investigations on electronic, elastic and thermodynamic properties of ZrC and ZrN under high pressure*. Mater. Chem. Phys. 129 (2011), pp. 99–104.
[30] P. Ojha, M. Aynyas and S.P. Sanyal, *Pressure-induced structural phase transformation and elastic properties of transition metal mononitrides*. J. Phys. Chem. Solids 68 (2007), pp. 148–152.
[31] W. Chen and J.Z. Jiang, *Elastic properties and electronic structures of 4d-and 5d-transition metal mononitrides*. J. Alloys Comp. 499 (2010), pp. 243–254.
[32] C. Stampfl, W. Mannstadt, R. Asahi and A.J. Freeman, *Electronic structure and physical properties of early transition metal mononitrides: density-functional theory LDA, GGA, and screened-exchange LDA FLAPW calculations*. Phys. Rev. B 63 (2001), pp. 155106–155116.
[33] E.K. Abavare, M.K. Donkor, S.N. Dodoo, O. Akoto, F.K. Ampong, B. Kwaakye-Awuah and R.K. Nkum, *Indirect phase transition of refractory nitrides compounds of: TiN, ZrN and HfN crystal structures*. Comput. Mater. Sci. 137 (2017), pp. 75–84.
[34] V.I. Ivashchenko, P.E.A. Turchi and V.I. Shevchenko, *Phase transformation B1 to B2 in TiC, TiN, ZrC and ZrN under pressure*. Condens. Matter Phys. 3 (2013), pp. 33602–33610.
[35] S.T. Weir, Y.K. Vohra and A.L. Ruoff, *High-pressure phase transitions and the equations of state of BaS and BaO*. Phys. Rev. B 33 (1986), pp. 4221–4226.
[36] G. Rousse, S. Klotz, A.M. Saitta, J. Rodriguez- Carvajal, M.I. McMahon, B. Couzinet and M. Mezouar, *Structure of the intermediate phase of PbTe at high pressure*. Phys. Rev. B 71 (2005), pp. 224116–224121.
[37] A.L. Ruoff, T. Li T, A.C. Ho, M.F. Pai, R.G. Greene, C. Narayana, J.C. Molstad, S.S. Trail, F.J. Jr. DiSalvo and P.E. van Camp, *Sevenfold coordinated MgSe: experimental internal atom position determination to 146 GPa, diffraction studies to 202 GPa, and theoretical studies to 500 GPa*. Phys. Rev. Lett. 81 (1998), pp. 2723–2726.
[38] M. Durandurdu, *High-pressure phase transitions of TiN: an ab initio constant pressure study*. Philos. Mag. 95 (2015), pp. 2376–2384.
[39] J.G. Zhao, L.X. Yang, Y. Yu, S.J. You, R.C. Yu, F.Y. Li, L.C. Chen, C.Q. Jin, X.D. Li, Y.C. Li and J. Liu, *Isostructural phase transition of TiN under high pressure*. Chin. Phys. Lett. 22 (2005), pp. 1199–1201.
[40] A.D. Becke, *Density functional exchange energy approximation with correct asymptotic behavior*. Phys. Rev. A 38 (1988), pp. 3098–3100.
[41] C. Lee, W. Yang and R.G. Parr, *Development of the Colle-Salvetti correlation-energy formula into a functional of the electron density*. Phys. Rev. B 37 (1988), pp. 785–789.
[42] N. Troullier and J.M. Martins, *Efficient pseudopotentials for plane-wave calculations*. Phys. Rev. B 43 (1991), pp. 993–2006.
[43] P. Ordejón, E. Artacho and J.M. Soler, *Self-consistent order-N density-functional calculations for very large systems*. Phys. Rev. B 53 (1996), pp. R10441–R10444.
[44] M. Parrinello and A. Rahman, *Polymorphic transitions in single crystals: A new molecular dynamics method*. J. Appl. Phys. 52 (1981), pp. 7182–7190.
[45] H.J. Monkhorst and J.D. Pack, *Special points for Brillouin-zone integrations*. Phys. Rev. B 13 (1976), pp. 5188–5192.
[46] R. Hundt, J.C. Schön, A. Hannemann and M. Jansen, *Determination of symmetries and idealized cell parameters for simulated structures*. J. Appl. Crystallogr. 32 (1999), pp. 413–416.
[47] S. Zhang and N.-X. Chen, *Molecular dynamics simulations for high-pressure induced B1–B2 transition in NaCl by möbius pair potentials*, Model. Simul. Mater. Sci. Eng. 11 (2003), pp. 331–338.

[48] D.M. Teter, *Computational alchemy: The search for new superhardmaterials*. Mrs. Bull., 23 (1998), pp. 22–27.
[49] X.Q. Chen, H. Niu, D. Li and Y. Li, *Modeling hardness of polycrystalline materials and bulk metallic glasses*. Intermetallics 19 (2011), pp. 1275–1281.
[50] Y. Tian, B. Xu and Z. Zhao, *Microscopic theory of hardness and design of novel superhard crystals*. Int. J. Refract. Met. Hard Mater. 33 (2012), pp. 93–106.